

## Enantioselective Catalysis

## Highly Enantioselective Iridium(I)-Catalyzed Hydrocarbonation of Alkenes: A Versatile Approach to Heterocyclic Systems Bearing Quaternary Stereocenters

Andrés Arribas, Martín Calvelo<sup>+</sup>, David F. Fernández<sup>+</sup>, Catarina A. B. Rodrigues, José L. Mascareñas, and Fernando López\*

**Abstract:** We report a versatile, highly enantioselective intramolecular hydrocarbonation reaction that provides a direct access to heteropolycyclic systems bearing chiral quaternary carbon stereocenters. The method, which relies on an iridium(I)/bisphosphine chiral catalyst, is particularly efficient for the synthesis of five-, six- and seven-membered fused indole and pyrrole products, bearing one and two stereocenters, with enantiomeric excesses of up to >99%. DFT computational studies allowed to obtain a detailed mechanistic profile and identify a cluster of weak non-covalent interactions as key factors to control the enantioselectivity.

## Introduction

The enantioselective formation of C–C bonds using metal-catalyzed C–H bond activations constitutes a major goal in modern organic synthesis.<sup>[1]</sup> In particular, processes involving the asymmetric addition of C(sp<sup>2</sup>)–H bonds across alkenes (i.e. hydrocarbonations) are highly attractive, owing to their simplicity, transformative power and full atom-economy.<sup>[2]</sup> In recent years there have been important advances in this endeavor, however, highly enantioselective approaches are still mostly limited to intermolecular processes.<sup>[3]</sup> Most of these reactions involve a directed insertion of a low-valent transition metal into a specific C(sp<sup>2</sup>)–H bond, leading to metal-hydride intermediates (**I**) that evolve to the

How to cite: *Angew. Chem. Int. Ed.* **2021**, *60*, 19297–19305  
International Edition: doi.org/10.1002/anie.202105776  
German Edition: doi.org/10.1002/ange.202105776

addition product through an alkene insertion/reductive elimination sequence (Scheme 1, eq. 1).<sup>[3]</sup>

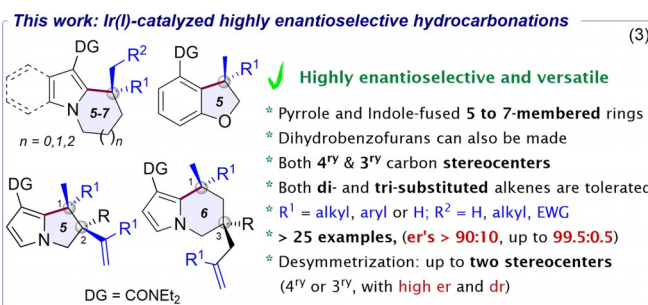
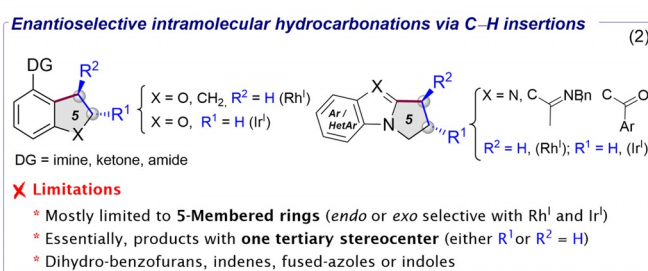
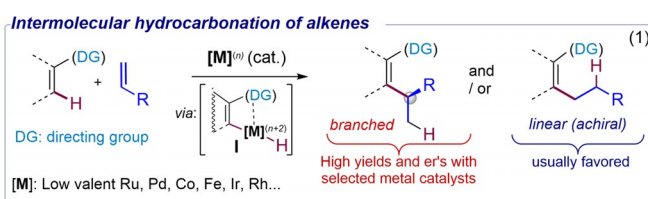
Translating this technology to intramolecular sceneries is very appealing, owing to the possibility of gaining a rapid and practical access to enantioriched, complex (poly)cyclic skeletons from readily available precursors. However, progress in this matter has been slow, and the asymmetric methods so far developed present a yet limited scope and versatility.<sup>[2]</sup> Indeed, state-of-the-art, highly enantioselective strategies based on Rh<sup>I</sup> and Ir<sup>I</sup> chiral catalysts are essentially limited to hydroarylation reactions,<sup>[4]</sup> and mostly deliver five-membered rings exhibiting one single tertiary stereocenter (Scheme 1, eq. 2).<sup>[5]</sup> On the other hand, mechanistically dissimilar hydrocarbonations promoted by high valent Rh<sup>III</sup> or Ru<sup>II</sup> catalysts, which proceed through carbometallation/protonation events instead of C–H oxidative insertions, are

[\*] A. Arribas, M. Calvelo,<sup>[†]</sup> D. F. Fernández,<sup>[†]</sup> C. A. B. Rodrigues, Prof. J. L. Mascareñas, Dr. F. López  
Centro Singular de Investigación en Química Biolóxica e Materiais Moleculares (CiQUS) and Departamento de Química Orgánica, Universidade de Compostela  
15782 Santiago de Compostela (Spain)  
E-mail: fernando.lopez.garcia@usc.es  
Dr. F. López  
Misión Biológica de Galicia, Consejo Superior de Investigaciones Científicas (CSIC)  
36080 Pontevedra (Spain)  
E-mail: fernando.lopez@csic.es

[†] These authors contributed equally to this work.

Supporting information and the ORCID identification number(s) for the author(s) of this article can be found under:  
https://doi.org/10.1002/anie.202105776.

© 2021 The Authors. Angewandte Chemie International Edition published by Wiley-VCH GmbH. This is an open access article under the terms of the Creative Commons Attribution Non-Commercial NoDerivs License, which permits use and distribution in any medium, provided the original work is properly cited, the use is non-commercial and no modifications or adaptations are made.



**Scheme 1.** Transition-Metal Catalyzed Hydrocarbonations of Alkenes via C–H Bond Activations.

also scarce and limited to the formation of five-membered rings.<sup>[6,7]</sup>

Therefore, despite the progress, there are a number of key challenges that remain to be addressed in order these cyclization technologies can truly impact the field of asymmetric synthesis. Some of these include: 1) the enantioselective assembly of cyclic products with diverse ring sizes (e.g. 5- to 7-membered rings), 2) the generation of products with more than one stereocenter, with high diastereo- and enantioselectivities, and 3) the construction of challenging all-carbon quaternary stereocenters from different types of precursors.<sup>[8,9]</sup> Moreover, of special significance would be to solve all these issues with a truly versatile method, in the context of building different types of relevant heterocyclic targets.

Among different heterocyclic systems, pyrroles and indoles are especially appealing, as they form the main structural core of a myriad of bioactive polycyclic products, like those shown in Figure 1.<sup>[10]</sup> Many of these products exhibit one or more stereocenters, including all-carbon quaternary centers. Despite important advances in the asymmetric synthesis of these heterocyclic scaffolds, catalytic, highly enantioselective methods for their direct assembly remain very scarce.<sup>[11]</sup>

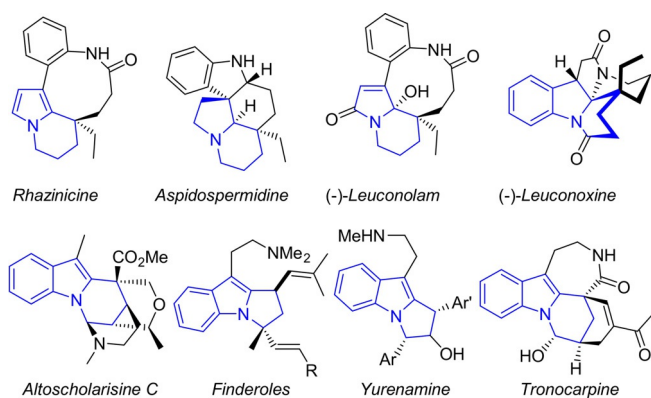


**Figure 1.** Natural Products Bearing Pyrrole or Indole Cores.

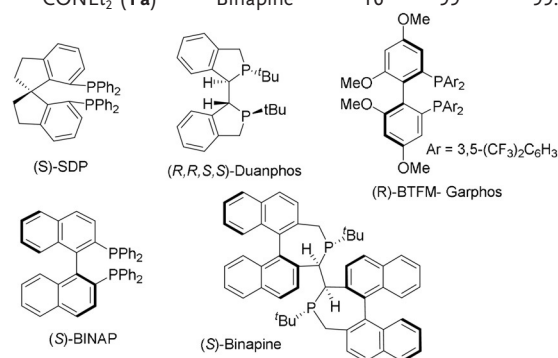
We report herein a robust and versatile cycloisomerization methodology to build a variety of pyrrole and indole-containing polycycles, featuring tertiary and all-carbon quaternary stereocenters, in a highly enantioselective manner (Scheme 1, eq. 3). The method relies on selected chiral iridium(I) catalysts that allow an efficient C–H activation process while providing for a highly enantioselective hydrocarbonation of a tethered alkene. The reaction tolerates different lengths in the tether connecting the reactants, so that five- six- and even seven-membered fused rings can be easily installed with very high er's. Very importantly, by using precursors that bear prochiral carbon centers, we show that it is possible to couple the hydrocarbonation with a concomitant desymmetrization. Thus, a variety of pyrrole-fused scaffolds bearing either vicinal or skipped stereocenters are obtained with very good diastereo- and enantioselectivities. Finally, we also include computational (DFT) studies that provide relevant mechanistic details and shed light on the key factors that determine the observed stereoselectivities.

## Results and Discussion

Our initial experiments were focused on pyrrole precursors owing the scarce number of methods for their highly enantioselective C(2)-H functionalization,<sup>[7a,11c]</sup> and the relevance of the cyclized products. Therefore, we selected pyrroles with *N*-tethered alkenyl chains of type **1** as initial substrates (Table 1 and Tables S1–S3). We first analyzed the performance of chiral iridium(I) complexes that had provided moderate enantioselectivities in our recently developed intramolecular hydroalkenylation reactions (Table 1, entries 1–3).<sup>[4b]</sup> Heating at 60 °C a dioxane solution of **1a** and the complex generated in situ from [Ir(COD)<sub>2</sub>]BARF and the spirobisphosphine (*S*)-SDP, led to a moderate conversion (50% approx) after 16 h. The 2,3-dihydropyrrolizine product **2a**, resulting from a 5-*exo* selective cyclization, was isolated in 44% yield, with a moderate 71:29 er (entry 1). The use of (*R,R,S,S*)-Duanphos allowed to improve the yield of **2a**, although the er remained modest (entry 2). Neither the *endo* regioisomer nor any other cyclized product were detected in these crude mixtures. The use of (*R*)-BTfM-Garphos or (*S*)-BINAP as ligands led to more efficient processes, providing

**Table 1:** Preliminary Analysis of the Ir-Catalyzed Enantioselective Hydroarylation of **1**.<sup>[a]</sup>

Entry	R (1)	L*	Time [h]	Yield <sup>[b]</sup> [%]	er <sup>[c]</sup>
1	CONEt <sub>2</sub> ( <b>1a</b> )	SDP	16	44	71:29
2	CONEt <sub>2</sub> ( <b>1a</b> )	Duanphos	16	81	71:29
3	CONEt <sub>2</sub> ( <b>1a</b> )	BTfM-Garphos	16	94	96:4
4	CONEt <sub>2</sub> ( <b>1a</b> )	BINAP	16	83	97:3
5	CONEt <sub>2</sub> ( <b>1a</b> )	Binapine	2	95	> 99.5:0.5
6 <sup>[d]</sup>	COMe ( <b>1a'</b> )	Binapine	16	49	65:35
7	H ( <b>1a''</b> )	Binapine	16	0	–
8 <sup>[e]</sup>	CONEt <sub>2</sub> ( <b>1a</b> )	Binapine	16	< 3	–
9 <sup>[f]</sup>	CONEt <sub>2</sub> ( <b>1a</b> )	Binapine	16	99	99.9:0.1



[a] Conditions: **1** was added to a solution of [Ir(COD)<sub>2</sub>]BARF (5 mol%) and L\* (5 mol%) in dioxane, and heated at 60 °C for the indicated time, unless otherwise noted. [b] Isolated yields; [c] er's determined by HPLC or SFC with chiral stationary phases. [d] Carried out with 10 mol% of (*S*)-Binapine at 120 °C (sealed tube). [e] Carried out using [Rh(COD)<sub>2</sub>]BARF instead of [Ir(COD)<sub>2</sub>]BARF. [f] Carried out with 1 mol% of the Ir/Binapine catalyst.

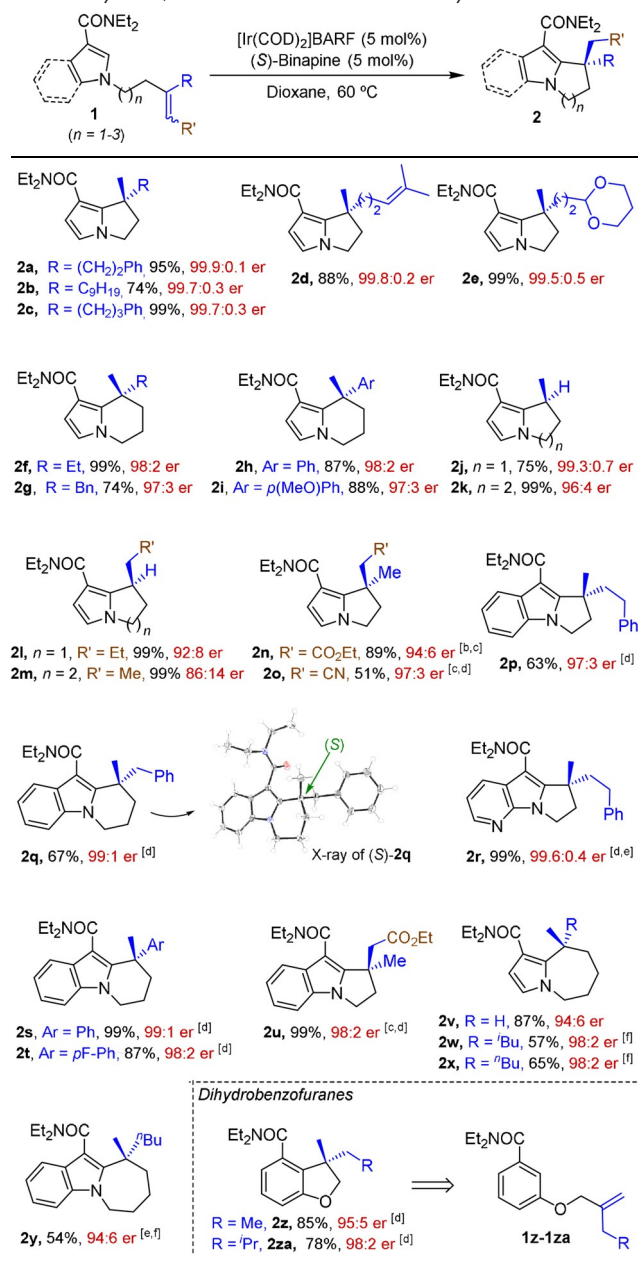
good yields of **2a** and er's up to 97:3 (entries 3 and 4).<sup>[12]</sup> Notably, during the screening process we eventually discovered that the Ir complex obtained from (*S*)-Binapine, a chiral bisphosphine that holds axial and central chirality (both at carbon and phosphorus), was even more effective in the hydrocarbonation of **1a**, delivering **2a** in 95% yield and with an almost perfect enantiomeric ratio, >99.5:0.5 (entry 5).<sup>[13]</sup>

Under otherwise identical reaction conditions, the cyclization of the pyrrole **1a'**, which holds a methyl ketone at C-3, instead of the diethyl carboxamide, required heating at 120 °C and a higher catalyst loading to achieve full conversion, while the corresponding product (**2a'**) was obtained with both moderate yield and er (65:35 er, entry 6). The relevance of the amide directing group was further stressed by the failing of the C-3 unsubstituted pyrrole **1a''** to provide any product, even after several hours at high temperatures (entry 7).<sup>[14]</sup> Noticeably, the Rh<sup>I</sup> complex analog to the above iridium catalyst did not afford any product in the reaction of **1a**, at 60 °C, and only traces of **2a** could be detected after prolonged heating at 120 °C (entry 8).

Overall, these results highlight the superiority of the Ir/Binapine catalyst, in combination with the carboxamide directing group, for promoting the enantioselective cyclization of the alkenyl pyrrol **1a**. Indeed, we were pleased to observe that this model reaction can be carried out with just 1 mol% of the Ir/Binapine catalyst, without deterring the yield or the enantiomeric ratio of the product, **2a** (entry 9).

With the optimal conditions in hand, we explored the scope of the process. The reaction of pyrroles **1b–1e**, bearing different types of substituents at the internal position of the alkene, was equally successful, providing the corresponding dihydro-1*H*-pyrrolizine products **2b–2e**, resulting from a completely selective 5-*exo* cyclization, in very good yields and with er's above 99.5:0.5 (Table 2). Chiral tetrahydroindolizines can also be efficiently assembled through an *exo*-like cyclization by using precursors with one additional methylene in the tether. Thus, products **2f–2i**, bearing all-carbon quaternary stereocenters, either with aryl or alkyl substituents, were obtained in good yields (74–99%) and with excellent enantiomeric ratios that range from 97:3 to 98:2. In these cases, the use of Binapine is critical to obtain good er's, as other chiral ligands that were effective with **1a**, such as BINAP, probed to be inefficient (er's < 60:40).<sup>[14]</sup> The method is not restricted to the construction of quaternary carbon stereocenters. Indeed, the cyclizations of precursors **1j** and **1k**, bearing monosubstituted alkenes, take place to give the expected products with tertiary stereocenters (**2j–k**), in high yields and excellent er's (up to 99.3:0.7). Precursors with 1,2-disubstituted alkenes, such as (*E*)-**1l** and (*E*)-**1m** also participated in the reaction providing the corresponding adducts, **2l** and **2m**, in quantitative yields and with high er's. Importantly, the use of trisubstituted alkenes, which has very few precedents in intramolecular hydrocarbonation processes,<sup>[2]</sup> is also tolerated. Thus, the hydrocarbonations of the precursors **1n** and **1o**, which both consist of a ≈1:1 *E/Z* mixture as a result of an unselective Wittig–Horner reaction,<sup>[14]</sup> proceeded smoothly at slightly higher temperatures, to deliver their corresponding adducts (**2n** and **2o**) with good yields and excellent enantiomeric ratios, of 94:6 and 97:3,

**Table 2:** *Exo*-Selective Enantioselective Hydrocarbonation of Alkene-Tethered Pyrroles, Indoles and Related Aromatic Systems.<sup>[a]</sup>



[a] Conditions: **1** was added to a solution of [Ir(COD)<sub>2</sub>]BARF (5 mol%) and (*S*)-Binapine (5 mol%) in dioxane, and the mixture was heated at 60 °C for 1–16 h (see the Supp. Info. for reaction times), unless otherwise noted; Isolated yields after chromatography; er's determined by HPLC or SFC. R' = H unless otherwise noted. [b] Carried out at 80 °C using 10 mol% of catalyst. [c] The corresponding precursor consist of a ≈1:1 *E/Z* mixture. [d] Carried out at 100 °C using 10 mol% of catalyst. [e] Reaction time 48 h. [f] Carried out at 100 °C using [Ir(COD)<sub>2</sub>]BARF / (*S*)-BINAP (10 mol%).

respectively. To the best of our knowledge, the possibility of obtaining the desired products with high *ee*, regardless of the configuration of the parent trisubstituted alkene, lacks precedents in related C–H hydrocarbonation protocols.

Indoles are also good substrates for the reaction, although a higher temperature is usually required to achieve full

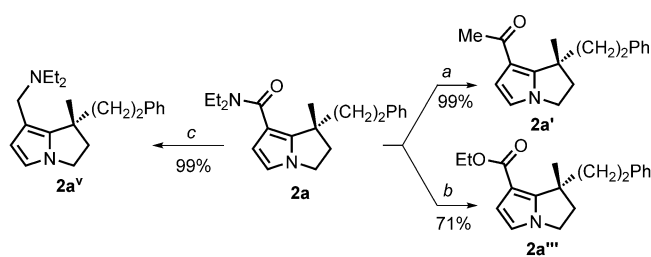
conversions. Therefore, dihydropyrrolo[1,2-*a*]indole and tetrahydropyrrolo[1,2-*a*]indole products **2p** and **2q** were both obtained in good yields and with er's above 97:3. The use of Binapine was also critical in these cases to achieve high er's.<sup>[14]</sup> Gratifyingly, the absolute configuration of **2q** (99:1 er) could be determined by X-ray crystallographic analysis.<sup>[14,15]</sup> Moreover, the 7-azaindole precursor **1r** also participated in the process to afford the corresponding dihydropyrrolopyrrolizine derivative **2r** in 99% yield and 99.6:0.4 er. Likewise, indole precursors with aryl substituents at the internal position of the alkene moiety are also good substrates for the Ir/Binapine catalyst, so that the tricyclic products **2s** and **2t** were obtained with high yields and er's  $\geq 98:2$ . An equally high enantiomeric ratio was also obtained in the cyclization of an indole precursor bearing a trisubstituted alkene (**1u**, *E/Z*  $\approx 1:1$ ), which afforded **2u** in 99% yield.

The robustness of the method allowed us to further extend the process to the synthesis of medium sized seven-membered fused rings, such as the tetrahydropyrrolo[1,2-*a*]azepine **2v**. Curiously, while the cyclization of **1v** was only found very effective using Binapine as ligand (87% yield and 94:6 er), the formation of related products with all-carbon quaternary stereocenters, such as **2w–2y**, through a 7-*exo* cyclization of the corresponding precursors, proceeded in better yields with BINAP (er's from 94:6 to 98:2). Overall, our method represents the first enantioselective metal-catalyzed cycloisomerization based on a C–H activation that allows to build either five-, six- or seven-membered rings, with excellent er's, regardless of the nature of the generated stereocenter.

Considering this versatility, we wondered whether the method could also be applied to the synthesis of dihydrobenzofurans, since most of the current asymmetric methods towards these systems are limited to the generation of tertiary stereocenters.<sup>[16]</sup> In this regard, we were pleased to observe that the catalyst generated from [Ir(COD)<sub>2</sub>]BARF and (*S*)-Binapine promoted the cyclization of *O*-alkenyl tether carboxamides **1z–1za** to provide the desired dihydrobenzofurans (**2z–2za**) in good yields and with excellent er's (up to 98:2). Therefore, this method can be ranked upon the most versatile enantioselective approaches towards different polyheterocyclic systems exhibiting all-carbon quaternary stereocenters.

While the dialkylamide could be perceived as a useless pendant, required for the C–H activation, it should be rather viewed as a useful handle for further manipulations. Thus, exemplified in a model product (**2a**), it can be directly transformed into a ketone (**2a'**), a carboxylic ester (**2a''**) or an amine (**2a<sup>v</sup>**) in good yields (Scheme 2).<sup>[14]</sup> Eventually, other elaborations could be proposed.

At this point we questioned whether this technology could be further adapted to build products containing multiple stereocenters at the newly generated ring, something that, in the context of asymmetric hydroarylations, has never been achieved efficiently.<sup>[2]</sup> Considering the *exo*-selective nature of the current cyclization, we envisioned that this goal could be approached by combining the cycloisomerization with a concomitant desymmetrization.<sup>[17]</sup> Therefore, we designed prochiral 1,4- and 1,6-diene precursors of type **3** (Table 3), which are very easy to make from readily available materials.<sup>[18]</sup>



**Scheme 2.** Preliminary exploration of the synthetic versatility of the carboxamide group in a model product. Conditions:<sup>[14]</sup> a) MeLi (excess); b) Et<sub>3</sub>O·BF<sub>4</sub>, Na<sub>2</sub>HPO<sub>4</sub>; c) LiAlH<sub>4</sub>, 50 °C.

Gratifyingly, treatment of **3a** with [Ir(COD)<sub>2</sub>]BARF/(*S*)-Binapine at 60 °C provided the expected dihydro-1*H*-pyrrolopyrrolizine product **4a** in 75% yield and an excellent 95:5 enantiomeric ratio (Table 3, entry 1). Increasing the temperature to 80 °C allowed to improve the yield to 90% without detrimental effects in the er (entry 2). The analog precursor **3b**, bearing an ethyl instead of a methyl group at the internal position of the alkene also gave the desired product, in this case bearing two stereocenters, as a 9:1 mixture of diastereoisomers. Interestingly, both the major (**4b**) and minor (**4b'**) isomers were obtained with excellent er's, of 98:2 and 95:5, respectively (entry 3). This result confirms the ability of the chiral catalyst to differentiate the enantiotopic alkenes of the prochiral center while ensuring the alkene facial selectivity.

The desymmetrizing strategy can also be applied to the hydroxyl-free precursor **3c**, which gave the desired tetrahydroindolizine product bearing two vicinal stereocenters with good dr (**4c**:**4c'** = 8:2) and excellent enantiomeric ratios (99.7:0.3 and 95:5, respectively, entry 4). Moreover, as shown in entries 5–7, the hydroarylation of prochiral pyrroles bearing a 1,6-diene was also feasible. Thus, the desymmetrizing hydrocarbonation of **3d** provided the tetrahydroindolizine derivative **4d**, with a good enantiomeric ratio (91:9) and 85% yield (entry 5). The cyclization of pyrrole **3e**, with a phenyl group at the internal position of the alkene provided the desired product, **4e**, bearing two fully substituted stereocenters in relative 1,3-positions, with complete diastereoselectivity, 95% yield and with an excellent er of 97:3 (entry 6). The generation of tertiary stereocenters is also possible. Thus, the tetrahydroindolizine derivative **4f** was obtained in 93% yield, with complete diastereoselectivity and 92:8 er (entry 7). The relative and absolute stereochemistry of this product was determined by X-ray crystallography.<sup>[14]</sup> Finally, the desymmetrizing hydroarylation can be extended to indole precursors such as **3g**, to give the product **4g** with good stereoselectivities (dr 1:0; er = 94:6, entry 8). This result paves the way for the application of this method to the asymmetric synthesis of biorelevant indole alkaloids. Worth to note, the use of Binapine in these cyclizations was also essential to achieve high levels of both diastereo- and enantiocontrol.

Overall, these transformations represent pioneering examples of desymmetrizing hydroarylation reactions that enable a quite impressive increase in skeletal and stereochemical complexity.<sup>[17c]</sup> The resulting pyrrole-based polycyc-

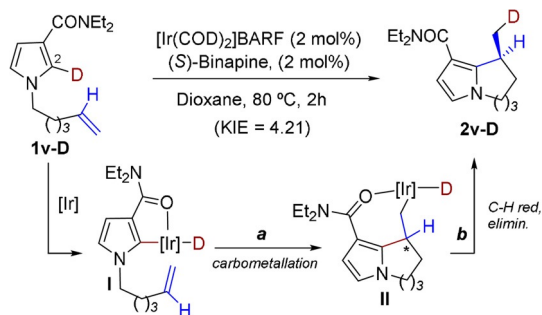
**Table 3:** Asymmetric Ir-Catalyzed Desymmetrizing Hydrocarbonylation of 1,4- and 1,6-Dienes of Type **3**.<sup>[a]</sup>

Entry	Precursor	R	<b>3</b>	Product ( <b>4</b> )	dr ( <b>4</b> : <b>4'</b> ) <sup>[b]</sup>	Yield [%] <sup>[c]</sup>	<b>4</b> , er <sup>[d]</sup>
1 <sup>[e]</sup>		Me	<b>3 a</b>		—	75	<b>4 a</b> , 95:5
2		Me	<b>3 a</b>		—	90	<b>4 a</b> , 95:5
3		Et	<b>3 b</b>		9:1	86	<b>4 b</b> , 98:2 <sup>[f,g]</sup>
4		—	<b>3 c</b>		8:2	93	<b>4 c</b> , 99.7:0.3 <sup>[g,h]</sup>
5		Me	<b>3 d</b>		—	85	<b>4 d</b> , 91:9
6		Ph	<b>3 e</b>		1:0	95	<b>4 e</b> , 97:3
7		H	<b>3 f</b>		1:0	93	<b>4 f</b> , 92:8
8		—	<b>3 g</b>		1:0	61	<b>4 g</b> , 94:6 <sup>[i]</sup>

[a] Conditions: **3** was added to a solution of [Ir(COD)<sub>2</sub>]BARF (10 mol%) and (S)-Binapine (10 mol%) in dioxane, and the mixture was heated at 80 °C for 16 h unless otherwise noted. [b] dr's determined by <sup>1</sup>H-NMR of the crude mixtures. [c] Isolated yields of **4** (and **4'**) after column chromatography. [d] er's determined by HPLC or SFC. [e] Carried out at 60 °C. [f] The minor isomer (**4b'**) is obtained with a 95:5 er.<sup>[14]</sup> [g] The relative configuration of **4** and **4'** were determined by NOE experiments.<sup>[14]</sup> [h] The minor isomer (**4c'**) is obtained with a 95:5 er.<sup>[14]</sup> [i] Carried out at 100 °C. After the hydroarylation process, the non-reactive allyl moiety isomerizes towards the observed internal alkene under reaction conditions.

lic products, bearing vicinal or skipped stereocenters, are obtained with high diastereo- and enantiomeric ratios.

From a mechanistic perspective, and based on previous work from our and other labs on Ir<sup>I</sup>-catalyzed hydrocarbonylations,<sup>[19]</sup> we postulate an initial oxidative addition of the C(2)–H bond of the (hetero)aryl moiety into the Ir<sup>I</sup>-biphosphine complex (**I**), followed by an *exo*-selective carbometallation (**II**) and a C–Ir–H reductive elimination. The formation of the deuterated product **2v-D** from the pyrrole **1v-D** is consistent with this scenario (Scheme 3).<sup>[20]</sup> Moreover, an experimentally determined kinetic isotope effect (KIE) of 4.2 strongly suggests the cleavage or the formation of a C–H bond is involved in the reaction turnover-limiting step.<sup>[14]</sup> The high enantioselectivities experimentally observed could be the result of an enantiofacial-selective migratory insertion of

**Scheme 3.** Mechanistic outline.

the alkene (*a*), followed by a stereochemically irrelevant C–H reductive elimination (*b*). Nonetheless, an alternative scenario based on reversible carbometallations followed by an enantiodiscriminating, rate-determining C–H reductive elimination cannot be fully ruled out. To discern between these options and shed light into the reasons behind the high enantioselectivities experimentally observed, we carried out a DFT analyses, using the model precursor **1g'** and the Ir<sup>I</sup>/(S)-Binapine complex (Figure 2 and Figures S44–S45).<sup>[21]</sup>

Our calculations indicate that, after coordination of the cationic iridium(I)/Binapine complex to the amide carbonyl moiety (**I-1**), there is an oxidative addition of the pyrrole C(2)–H bond to the Ir<sup>I</sup> center through an accessible energy barrier of 18.5 kcal mol<sup>−1</sup> (**TS-1**, Figure 2), leading to a distorted square-pyramidal iridium(III)-hydride species, **I-2**. Then, coordination of the olefin to the iridium center leads to two octahedral diastereoisomers (*pseudo*-enantiomers with respect to the metal center) which, remarkably, are energetically very different. In particular, species **I-3<sup>S</sup>**, which eventually will lead to the experimentally observed enantiomer (**S-2g'**) is 5.8 kcal mol<sup>−1</sup> more stable than its homologue **I-3<sup>R</sup>**, which would yield **R-2g'**.<sup>[22]</sup> Evaluation of the subsequent carbometallations indicates that the *exo*-selective migratory insertion from **I-3<sup>S</sup>**, proceeds through a transition state, **TS-3<sup>S</sup>**, which is 3.1 kcal mol<sup>−1</sup> more stable than that of the *R*-isomer (**TS-3<sup>R</sup>**). The resulting iridium(III) hydride intermediate **I-4<sup>S</sup>** is also significantly more stable than **I-4<sup>R</sup>**, by more than 3 kcal mol<sup>−1</sup> [ $\Delta\Delta G_{(I-4R-I-4S)} = 3.6$  kcal mol<sup>−1</sup>].

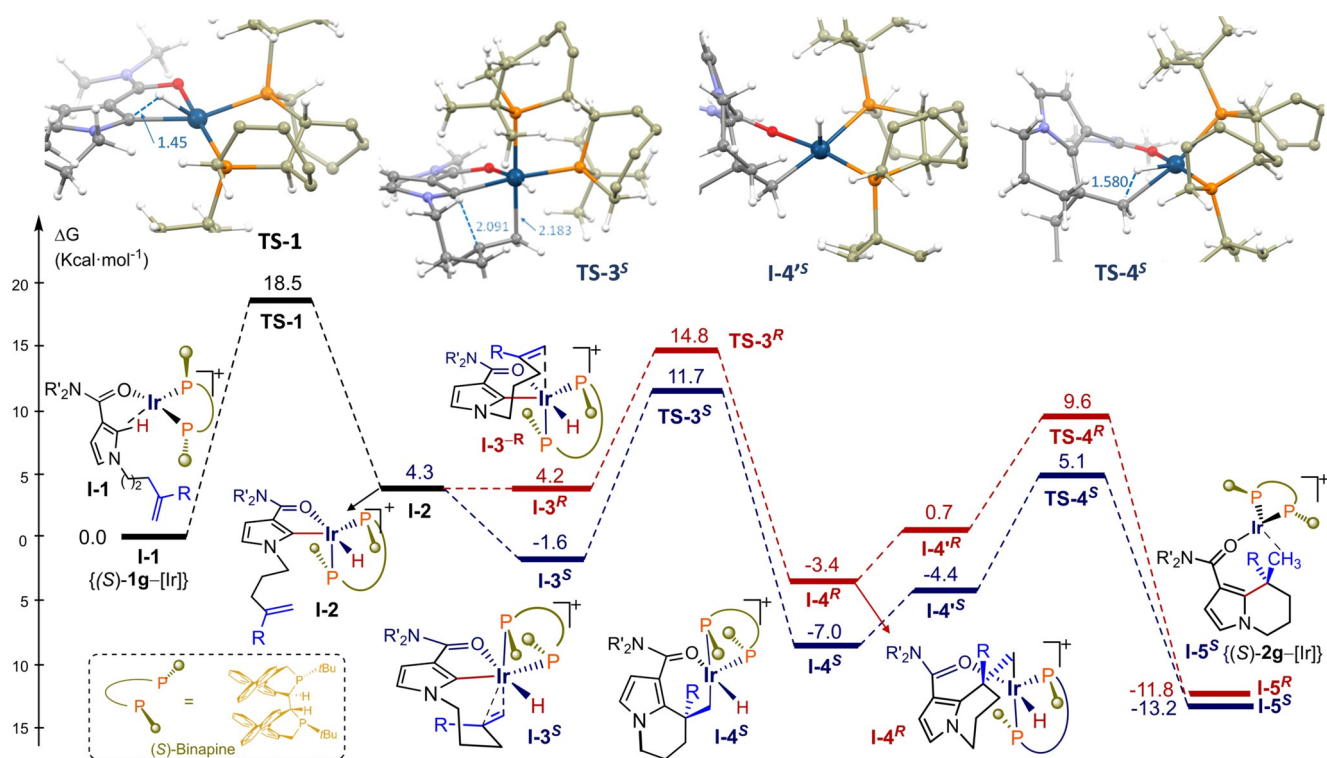


**Figure 2.** Energy Profile  $\Delta G^{\text{soln}}$  (kcal mol<sup>-1</sup>) for the Hydrocarbonation of **1g'** ( $R' = \text{Me}$ ,  $R = \text{Bn}$ ;  $[\text{Ir}] = [\text{Ir}(\text{Binapine})]^+$ ); B3LYP/6-31G(d) (LANL2DZ for Ir) // M06/6-311++g(d,p) (SDD for Ir).<sup>[21]</sup> Binapine ligand is mostly simplified in the 3D representations (aryl rings omitted) for clarity. Stationary points are truncated, for their full representations see the Supporting Information.

The C–H reductive elimination that closes the catalytic cycle entails an initial isomerization to a square-pyramidal isomer that holds the hydrogen in apical disposition (from **I-4** to **I-4'**), to facilitate the orbital interactions for the subsequent C–H bond forming process (**TS-4**). The overall energy barriers associated to the reductive elimination are similar for both isomers (12–13 kcal mol<sup>-1</sup>), being the one that delivers the experimentally observed enantiomer (**I-5<sup>S</sup>**) slightly favored, by 0.9 kcal mol<sup>-1</sup>. Thus, the corresponding transition state **TS-4<sup>S</sup>** lies 4.5 kcal mol<sup>-1</sup> below than that leading to the minor enantiomer. According to the energetic span model,<sup>[23]</sup> **TS-1** is the TOF-determining transition state (TDTS) and **I-1** the TOF-determining intermediate (TDI), resulting in an energetic span ( $\delta E$ ) of 18.5 kcal mol<sup>-1</sup>. Therefore, the theoretical results are in consonance with the experimental conditions as well as with the experimentally observed KIE, confirming that the C–H oxidative addition to the Ir<sup>I</sup> complex is turnover-determining. Moreover, the calculated energetic profile corroborates that the enantiodetermining step is the alkene migratory insertion ( $\Delta\Delta G = 3.1$  kcal mol<sup>-1</sup>), which is in full agreement with the high  $e_r$ 's experimentally obtained, as well as with the absolute configuration of the major enantiomer (e.g. *S-2g'*).

On the other hand, a preliminary DFT exploration of the desymmetrizing hydrocarbonation, using a model substrate analog to **3f** (**3f'**, see the Supporting Information), is also in qualitative agreement with the experimental results. Specifically, the computed data suggests that the observed selectivity at the desymmetrized center is related to an energetically preferred conformation at the iridacyclic stationary points **I-3**

and **TS-3**, which minimize 1,3-diaxial interactions by placing the less bulky hydroxyl group in axial disposition ( $\Delta\Delta G = 1.7$  kcal mol<sup>-1</sup>).<sup>[14]</sup> A related analysis with a second model precursor **3b'**, analog of **3b** (Table 3, entry 3), is also in accordance with the experimentally observed selectivity towards the dihydro-1*H*-pyrrolizine isomer **4b**.<sup>[14]</sup>

Finally, to shed some light into the reasons behind the high enantiofacial selectivities, we analyzed the non-covalent interactions (NCIs) involved in the enantiodetermining carbometallation step, using the NCI-index based on electron density (NCIPLOT program), as well as through the atoms in molecule (AIM) formalism, to identify the bond paths of these interactions and their bond critical points.<sup>[14,24]</sup> We first analyzed the intermediates **I-3<sup>S</sup>** and **I-3<sup>R</sup>** and found that the more stable isomer, **I-3<sup>S</sup>**, shows a higher number of stabilizing non-covalent interactions than **I-3<sup>R</sup>** (13 vs. 10 NCI's). Several of the found NCI's are equal or very similar between both diastereomeric intermediates (e.g. a C–H... $\pi$  interaction between a <sup>t</sup>Bu group of the ligand and the pyrrole ring, see Figure 3, interaction **g**; see also Figure S48 and Tables S6–S7). However, we have also found some key differences. In particular, **I-3<sup>S</sup>** holds three interactions between the carboxamide group at C-3 and the chiral ligand: two of them involve C–H...O contacts between the carbonyl oxygen and a <sup>t</sup>Bu group of Binapine, while the third one involves a related C–H...N interaction with the amide nitrogen (Figure 3, interactions **a–c**, respectively). Notably, the less stable isomer, **I-3<sup>R</sup>** only exhibits two of these interactions (Figure 3).<sup>[25]</sup>

Additionally, a second type of weak non-covalent attractive interactions, namely hydrogen-hydrogen bonding inter-

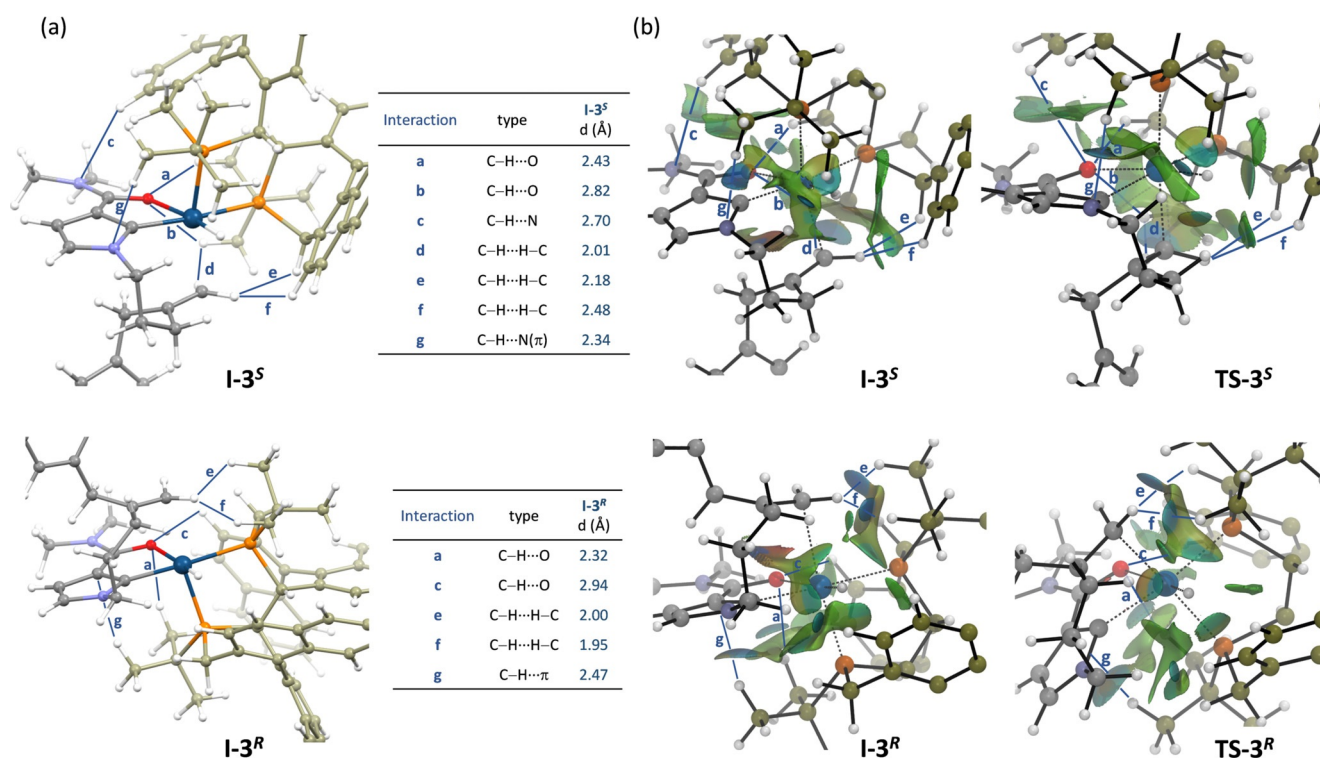


**Figure 3.** Optimized geometries of stationary points **I-3<sup>S</sup>**, **I-3<sup>R</sup>**, **TS-3<sup>S</sup>** and **TS-3<sup>R</sup>** highlighting: (a) key interatomic contacts at **I-3<sup>S</sup>** and **I-3<sup>R</sup>** (blue lines **a–g**), which correspond to non-covalent interactions (NCI's) for which bond paths and bond critical points were found by AIM formalism. The type of each interatomic interaction and the distance (Å) associated to them at **I-3<sup>R</sup>** and **I-3<sup>S</sup>** are tabulated; (b) NCIs obtained by NCIPLOT of **I-3<sup>S</sup>**, **I-3<sup>R</sup>** and their corresponding transition states **TS-3<sup>S</sup>** and **TS-3<sup>R</sup>** indicating the bond paths found by AIM (blue lines).<sup>[14]</sup> Iridium bonds are depicted with dot lines for clarity. Only selected fractions of the whole stationary points are shown.

actions of type C-H...H-C, was detected between the terminal hydrogen atoms of the alkene moiety and specific hydrogens of the ligand.<sup>[26]</sup> Thus, one of the olefinic hydrogens of **I-3<sup>S</sup>** shows a C-H...H-C interaction with a <sup>t</sup>Bu group of Binapine (Figure 3, interaction **d**), while the other alkenyl hydrogen establishes two of these contacts with two different hydrogens of the ligand (interactions **e** and **f**). Notably, in species **I-3<sup>R</sup>**, only one of the alkene hydrogens establishes C-H...H-C interactions, resulting in a lower stabilization (interactions **e** and **f**, Figure 3). Moreover, the high directionality of two of the C-H...H-C interactions in **I-3<sup>S</sup>** (**d** and **e**), which are essentially coplanar, might further contribute to its stability. Worth to note, related homopolar C-H...H-C interactions have been scarcely discussed in organometallic complexes and, to the best of our knowledge, they have not been previously proposed as key enantiodiscriminating factors.<sup>[27,28]</sup>

Regarding the ensuing transition states, the most stable one, **TS-3<sup>S</sup>**, holds a slightly reduced number of NCIs compared to its respective precursor intermediate, **I-3<sup>S</sup>**. However, all the C-H...O and C-H...H-C contacts previously identified in **I-3<sup>S</sup>** are somehow preserved in the transition state (**TS-3<sup>S</sup>**, see Figure 3). Likewise, **TS-3<sup>R</sup>** also keeps the same key interactions than **I-3<sup>R</sup>**. Therefore, the same key factors which determine the higher stability of **I-3<sup>S</sup>** versus **I-3<sup>R</sup>** are responsible for the lower energy of **TS-3<sup>S</sup>** over **TS-3<sup>R</sup>**.

Overall, these data suggest that the high facial selectivity stems from additive and synergistic effect of several weak

non-covalent attractive interactions, particularly those between the carboxamide moiety and specific hydrogens of Binapine (C-H...O interactions), and between hydrogens of the olefin and the ligand (C-H...H-C dihydrogen interactions). In consonance with these results, the lower enantioselectivity observed in the annulation of **1a'**, might be associated to the presence of a methyl ketone at C-3, which is less coordinating than the dialkyl carboxamide (see Table 1, entry 6 and Table S2).<sup>[29]</sup>

## Conclusion

In summary, we have developed a highly enantioselective iridium-catalyzed intramolecular hydrocarbonation method that provides five-, six- and seven-ring fused heterocyclic scaffolds equipped with tertiary and all-carbon quaternary stereocenters. Both disubstituted and 1,1,2-trisubstituted alkenes are tolerated, enabling the formation of products containing different stereocenters and with a variety of substituents. Moreover, by using prochiral alkenyl pyrrole precursors, the method allows a very efficient desymmetrization, yielding a variety of tetrahydroindolizine and dihydropyrrolizine derivatives bearing vicinal or skipped stereocenters with excellent levels of diastereo- and enantioselectivities. Finally, DFT computational studies confirm the carbometallation as the enantiodetermining step of the reaction and are fully consonant with the experimental observations.

Moreover, we identified key non-covalent interactions that allow to rationalize the high enantiofacial selectivity. Our discoveries pave the way for the design of novel hydrocarbonation processes using this type of chiral iridium catalysts.

### Acknowledgements

This work received financial support from the Spanish MINECO (SAF2016-76689-R, PID2019-108624RB-I00, CTQ2017-84767-P, PID2020-118579GB-I00), the Xunta de Galicia (ED431C 2017/19, 2015-CP082, Centro Singular de Investigación de Galicia accreditation 2019-2022, ED431G 2019/03, a predoctoral Fellowship to A. A. and M. C. and a postdoctoral Fellowship to D. F. F, ED481B-2019-005) and the ERDF, ERC (Adv. Grant No. 340055). The Orfeo-Cinca network (CTQ2016-81797-REDC), Alejandro Rey (preliminary contributions) and Dr. Rebeca García-Fandiño (helpful discussions) are also acknowledged.

### Conflict of Interest

The authors declare no conflict of interest.

**Keywords:** C-H activation · enantioselective · heterocycles · hydrocarbonation · iridium

- [1] For reviews, see: a) C. G. Newton, S. G. Wang, C. C. Oliveira, N. Cramer, *Chem. Rev.* **2017**, *117*, 8908–8976; b) Q. Shao, K. Wu, Z. Zhuang, S. Qian, J.-Q. Yu, *Acc. Chem. Res.* **2020**, *53*, 833–851; c) J. Loup, U. Dhawa, F. Pesciaioli, J. Wencel-Delord, L. Ackermann, *Angew. Chem. Int. Ed.* **2019**, *58*, 12803–12818; *Angew. Chem.* **2019**, *131*, 12934–12949; d) L. Woźniak, J. F. Tan, Q. H. Nguyen, A. Madron du Vigné, V. Smal, Y. X. Cao, N. Cramer, *Chem. Rev.* **2020**, *120*, 10516–10543; e) G. Liao, T. Zhang, Z. K. Lin, B. F. Shi, *Angew. Chem. Int. Ed.* **2020**, *59*, 19773–19786; *Angew. Chem.* **2020**, *132*, 19941–19954; f) S. Motevalli, Y. Sokeirik, A. Ghanem, *Eur. J. Org. Chem.* **2016**, 1459–1475.
- [2] For reviews covering this topic, see: a) Z. Dong, Z. Ren, S. J. Thompson, Y. Xu, G. Dong, *Chem. Rev.* **2017**, *117*, 9333–9403; b) D. F. Fernández, J. L. Mascareñas, F. López, *Chem. Soc. Rev.* **2020**, *49*, 7378–7405; c) D. A. Colby, R. G. Bergman, J. A. Ellman, *Chem. Rev.* **2010**, *110*, 624–655; d) F. Kakiuchi, S. Murai, *Acc. Chem. Res.* **2002**, *35*, 826–834; e) V. Ritleng, C. Sirlin, M. Pfeffer, *Chem. Rev.* **2002**, *102*, 1731–1770.
- [3] For selected recent examples of enantioselective intermolecular hydrocarbonations, see: a) A. Romero-Arenas, V. Hornillos, J. Iglesias-Sigüenza, R. Fernández, J. López-Serrano, A. Ros, J. M. Lassaletta, *J. Am. Chem. Soc.* **2020**, *142*, 2628–2639; b) S. Grélaud, P. Cooper, L. J. Feron, J. F. Bower, *J. Am. Chem. Soc.* **2018**, *140*, 9351–9356; c) Y. Ebe, M. Onoda, T. Nishimura, H. Yorimitsu, *Angew. Chem. Int. Ed.* **2017**, *56*, 5607–5611; *Angew. Chem.* **2017**, *129*, 5699–5703; d) J. S. Marcum, C. C. Roberts, R. S. Manan, T. N. Cervarich, S. J. Meek, *J. Am. Chem. Soc.* **2017**, *139*, 15580–15583; e) A. Whyte, A. Torelli, B. Mirabi, L. Prieto, J. F. Rodríguez, M. Lautens, *J. Am. Chem. Soc.* **2020**, *142*, 9510–9517; f) C. S. Sevov, J. F. Hartwig, *J. Am. Chem. Soc.* **2013**, *135*, 2116–2119; g) T. Shibata, T. Shizuno, *Angew. Chem. Int. Ed.* **2014**, *53*, 5410–5413; *Angew. Chem.* **2014**, *126*, 5514–5517; h) X. Vidal, J. L. Mascareñas, M. Gulías, *J. Am. Chem. Soc.* **2019**, *141*, 1862–1866; i) G. E. M. Crisenza, J. F. Bower, *Chem. Lett.* **2016**, *45*, 2–9; See also references 1d and 2a-b.
- [4] a) R. K. Thalji, J. A. Ellman, R. G. Bergman, *J. Am. Chem. Soc.* **2004**, *126*, 7192–7193; b) H. Harada, R. K. Thalji, R. G. Bergman, J. A. Ellman, *J. Org. Chem.* **2008**, *73*, 6772–6779; c) A. S. Tsai, R. M. Wilson, H. Harada, R. G. Bergman, J. A. Ellman, *Chem. Commun.* **2009**, 3910–3912; d) T. Shibata, N. Ryu, H. Takano, *Adv. Synth. Catal.* **2015**, *357*, 1131–1135; e) V. S. Shinde, M. V. Mane, L. Cavallo, M. Rueping, *Chem. Eur. J.* **2020**, *26*, 8308–8313; f) T. Shibata, H. Kurita, S. Onoda, K. S. Kanyiva, *Asian J. Org. Chem.* **2018**, *7*, 1411–1418; g) D. F. Fernández, M. Gulías, J. L. Mascareñas, F. López, *Angew. Chem. Int. Ed.* **2017**, *56*, 9541–9545; *Angew. Chem.* **2017**, *129*, 9669–9673.
- [5] Only a couple of isolated examples have been reported to provide six-membered rings, with ee's of 58 and 84% (refs. [4e] and [4d]), while only a single example on the formation of a carbon quaternary stereocenter has been reported with good yield and very high ee (ref. [4f]).
- [6] a) B. Ye, P. A. Donets, N. Cramer, *Angew. Chem. Int. Ed.* **2014**, *53*, 507–511; *Angew. Chem.* **2014**, *126*, 517–521; b) G. Li, Q. Liu, L. Vasamsetty, W. Guo, J. Wang, *Angew. Chem. Int. Ed.* **2020**, *59*, 3475–3479; *Angew. Chem.* **2020**, *132*, 3503–3507; c) Z. Y. Li, H. H. C. Lakmal, X. Qian, Z. Zhu, B. Donnadieu, S. J. McClain, X. Xu, X. Cui, *J. Am. Chem. Soc.* **2019**, *141*, 15730–15736.
- [7] Alternative hydrocarbonations based on related ligand-to-ligand hydrogen transfer processes have also been reported in enantioselective fashion with Ni<sup>0</sup> catalysts, but they are essentially restricted to the formation of six-membered rings bearing a single tertiary stereocenter, see: a) J. Diesel, D. Grosheva, S. Kodama, N. Cramer, *Angew. Chem. Int. Ed.* **2019**, *58*, 11044–11048; *Angew. Chem.* **2019**, *131*, 11160–11164; b) J. Loup, V. Muller, D. Ghorai, L. Ackermann, *Angew. Chem. Int. Ed.* **2019**, *58*, 1749–1753; *Angew. Chem.* **2019**, *131*, 1763–1767; c) W. B. Zhang, X. T. Yang, J. B. Ma, Z. M. Su, S. L. Shi, *J. Am. Chem. Soc.* **2019**, *141*, 5628–5634; For an exception with a Sc<sup>III</sup> catalyst, limited to (benzo)imidazoles, see: d) S. J. Lou, Z. Mo, M. Nishiura, Z. Hou, *J. Am. Chem. Soc.* **2020**, *142*, 1200–1205.
- [8] Organic molecules containing all-carbon-substituted quaternary stereocenters usually show unique bioactivities; therefore, the efficient and enantioselective construction of these stereocenters is a major goal that receives intensive attention, see: a) K. W. Quasdorf, L. E. Overman, *Nature* **2014**, *516*, 181–191; b) Y. Liu, S. J. Han, W. B. Liu, B. M. Stoltz, *Acc. Chem. Res.* **2015**, *48*, 740–751; c) R. Long, J. Huang, J. Gong, Z. Yang, *Nat. Prod. Rep.* **2015**, *32*, 1584–1601; d) Y. Li, S. Xu, *Chem. Eur. J.* **2018**, *24*, 16218–16245.
- [9] Regardless of the mechanism, only a couple of isolated cases involve the concomitant formation of two tertiary stereocenters (see ref. [7c] and [4b]), while highly enantioselective examples leading to all-carbon quaternary stereocenters are limited to alkyl-substituted dihydrobenzofuranes (refs. [6a,b]), (benz)imidazoles (ref. [7d]) and an isolated example of a  $\delta$ -lactone (ref. [4f]).
- [10] a) *Heterocycles in Natural Product Synthesis* (Eds.: K. C. Majumdar, S. K. Chattopadhyay), Wiley-VCH, Weinheim, **2011**, pp. 187–220; b) C. T. Walsh, S. Garneau-Tsodikova, A. R. Howard-Jones, *Nat. Prod. Rep.* **2006**, *23*, 517–531; c) J. Barluenga, C. Valdés, in *Modern Heterocyclic Chemistry*, Wiley-VCH, Weinheim, **2011**, pp. 377–531; d) J. Bergman, T. Janosik, in *Modern Heterocyclic Chemistry*, Wiley-VCH, Weinheim, **2011**, pp. 269–375; e) J. E. Saxton, *Nat. Prod. Rep.* **1997**, *14*, 559–590; f) M. Ishikura, T. Abe, T. Choshi, S. Hibino, *Nat. Prod. Rep.* **2015**, *32*, 1389–1471.
- [11] a) W. J. Olivier, J. A. Smith, A. C. Bissember, *Org. Biomol. Chem.* **2018**, *16*, 1216–1226; b) Z. Xu, Q. Wang, J. Zhu, *Chem.*



- Soc. Rev.* **2018**, *47*, 7882–7898; c) J. A. Schiffner, T. H. Wöste, M. Oestreich, *Eur. J. Org. Chem.* **2010**, 174–182; d) C. X. Zhuo, Q. F. Wu, Q. Zhao, Q. L. Xu, S. L. You, *J. Am. Chem. Soc.* **2013**, *135*, 8169–8172; e) Z. Xu, Q. Wang, J. Zhu, *J. Am. Chem. Soc.* **2013**, *135*, 19127–19130; f) G. Li, C. Piemontesi, Q. Wang, J. Zhu, *Angew. Chem. Int. Ed.* **2019**, *58*, 2870–2874; *Angew. Chem.* **2019**, *131*, 2896–2900; g) L. Huang, Y. Cai, C. Zheng, L.-X. Dai, S.-L. You, *Angew. Chem. Int. Ed.* **2017**, *56*, 10545–10548; *Angew. Chem.* **2017**, *129*, 10681–10684; h) C.-X. Zhuo, X. Zhang, S.-L. You, *ACS Catal.* **2016**, *6*, 5307–5310.
- [12] Unfortunately, these ligands did not provide equally high enantioselectivities in the cyclization of several other precursors of type **1** (vide infra).
- [13] To the best of our knowledge, this chiral ligand had never been shown successful in Ir<sup>I</sup> catalysis. For its development, see: a) W. Tang, W. Wang, Y. Chi, X. Zhang, *Angew. Chem. Int. Ed.* **2003**, *42*, 3509–3511; *Angew. Chem.* **2003**, *115*, 3633–3635; See also: b) *Encyclopedia of Reagents for Organic Synthesis*, Wiley, Hoboken, **2011**, <https://doi.org/10.1002/047084289X.rm01362>.
- [14] See the Supporting Information for further details.
- [15] We confirmed that several of these reactions (e.g. those leading to **2a–2e**, **2f** and **2g**), can be carried out with just 1–2 mol % of catalyst, delivering equally good er's and slightly reduced yields (5–15 % lower), although prolonged reaction times are required (2–48 h, see the Supporting information).
- [16] For two exceptions with high valent transition metal catalysts, see refs. [6a,b].
- [17] a) Due to this *exo* nature, the use of tri- or tetra-substituted alkenes would not increase the number of stereocenters at the newly formed ring system; b) Previous enantioselective hydroarylations had not been proven efficient for the asymmetric generation of cyclic products with multiple stereocenters, regardless of their mechanistic scenario; c) For an atroposelective intermolecular desymmetrization of biaryls, see ref. [3a].
- [18] For the use of prochiral 1,*n*-dienes in other desymmetric transition metal catalyzed processes, such as cross-couplings, ring closing metathesis or hydroacylations, see: a) X. P. Zeng, Z. Y. Cao, Y. H. Wang, F. Zhou, J. Zhou, *Chem. Rev.* **2016**, *116*, 7330–7396; b) F. Zhou, L. Zhu, B.-W. Pan, Y. Shi, Y.-L. Liu, J. Zhou, *Chem. Sci.* **2020**, *11*, 9341–9365; c) J. W. Park, K. G. Kou, D. K. Kim, V. M. Dong, *Chem. Sci.* **2015**, *6*, 4479–4483.
- [19] For a review covering mechanistic details, see ref. [2b]. For key references, see: a) G. Huang, P. Liu, *ACS Catal.* **2016**, *6*, 809–820; b) D. Xing, X. Qi, D. Marchant, P. Liu, G. Dong, *Angew. Chem. Int. Ed.* **2019**, *58*, 4366–4370; *Angew. Chem.* **2019**, *131*, 4410–4414; c) Y. Lang, M. Zhang, Y. Cao, G. Huang, *Chem. Commun.* **2018**, *54*, 2678–2681; d) D. F. Fernández, C. A. B. Rodrigues, M. Calvelo, M. Gullías, J. L. Mascareñas, F. López, *ACS Catal.* **2018**, *8*, 7397–7402.
- [20] An alternative scenario based on a hydrometallation/C–C reductive elimination sequence is less likely since C–Ir–C reductive eliminations are generally impeded by the high strength of the Ir–C bonds, thus favoring reversibility towards the carbometallation/C–H reductive elimination pathway. See refs. [2b] and [19] for further details.
- [21] DFT calculations have been carried out with Gaussian 09. The geometries of all species were optimized using the B3LYP hybrid functional together with the 6-31G(d) basis set for C, H, O, P and N and the LANL2DZ basis set for Ir. Single-point calculations of the optimized systems were carried out using the hybrid functional M06 together with the 6-311++g(d,p) basis set for C, H, O, P and N, and the Stuttgart-Dresden (SDD) ECP for Ir, in dioxane (using SMD model). See the Supp. Info. for further details.
- [22] We found that these two octahedral isomers, which hold the carbonyl and hydride in *trans* disposition, are significantly more stable than other isomers that hold the hydride *trans* to a phosphorus atom or to the C(2) pyrrole atom.
- [23] S. Kozuch, S. Shaik, *Acc. Chem. Res.* **2011**, *44*, 101–110.
- [24] a) E. R. Johnson, S. Keinan, P. Mori-Sánchez, J. Contreras-García, A. J. Cohen, W. Yang, *J. Am. Chem. Soc.* **2010**, *132*, 6498–6506; b) R. Parthasarathi, V. Subramanian, N. Sathya-murthy, *J. Phys. Chem. A* **2006**, *110*, 3349–3351; c) M. Prakash, G. K. Samy, V. Subramanian, *J. Phys. Chem. A* **2009**, *113*, 13845–13852.
- [25] a) K. B. Moore III, K. Sadeghian, C. D. Sherrill, C. Ochsenfeld, H. F. Schaefer III, *J. Chem. Theory Comput.* **2017**, *13*, 5379–5395; b) R. Taylor, O. Kennard, *J. Am. Chem. Soc.* **1982**, *104*, 5063–5070; c) Y. Wang, Y. Qiao, D. Wei, M. Tang, *Org. Chem. Front.* **2017**, *4*, 1987–1998.
- [26] These dispersion-dominated stabilizing C–H...H–C interactions are proposed to involve both London dispersions forces and a certain degree of covalent-charge delocalization to the interatomic H–H region, see: a) C. F. Matta, J. Hernandez-Trujillo, T. H. Tang, R. F. Bader, *Chem. Eur. J.* **2003**, *9*, 1940–1951; b) J. Echeverría, G. Aullon, D. Danovich, S. Shaik, S. Alvarez, *Nat. Chem.* **2011**, *3*, 323–330; c) M. P. Mitoraj, F. Sagan, M. G. Babashkina, A. Y. Isaev, Y. M. Chichigina, D. A. Safin, *Eur. J. Org. Chem.* **2019**, 493–503; For a review on the importance of synergistic London dispersion interactions, see: d) J. P. Wagner, P. R. Schreiner, *Angew. Chem. Int. Ed.* **2015**, *54*, 12274–12296; *Angew. Chem.* **2015**, *127*, 12446–12471.
- [27] For selected cases of achiral organometallic compounds wherein these interactions have been proposed, see: a) S. Thakur, M. G. B. Drew, A. Franconetti, A. Frontera, S. Chattopadhyay, *RSC Adv.* **2019**, *9*, 35165–35175; b) S. N. Britvin, A. M. Rummyantsev, A. A. Silyutina, M. V. Padkina, *ChemistrySelect* **2017**, *2*, 8721–8725; c) D. A. Safin, M. G. Babashkina, K. Robeyns, M. P. Mitoraj, P. Kubisiak, Y. Garcia, *Chem. Eur. J.* **2015**, *21*, 16679–16687.
- [28] For selected examples showing the participation of different weak NCI's in enantioselection processes, see: a) A. A. Thomas, K. Speck, I. Kevlishvili, Z. Lu, P. Liu, S. L. Buchwald, *J. Am. Chem. Soc.* **2018**, *140*, 13976–13984; b) A. J. Neel, M. J. Hilton, M. S. Sigman, F. D. Toste, *Nature* **2017**, *543*, 637–646; c) E. H. Krenske, K. N. Houk, *Acc. Chem. Res.* **2013**, *46*, 979–989.
- [29] In consonance with these results, a DFT analysis on a model precursor **1g<sub>Me</sub>**, bearing a methyl ketone at C-3 instead of the carboxamide, confirms that the  $\Delta\Delta G$  of the enantiodiscriminating carbometallation step [ $\Delta G(\text{TS-3}_{\text{Me}}^{\text{R}}) - \Delta G(\text{TS-3}_{\text{Me}}^{\text{S}})$ ] is significantly reduced, down to 1 kcal mol<sup>-1</sup> (see the Supp. Info. Figure S49).

Manuscript received: April 28, 2021

Revised manuscript received: June 10, 2021

Accepted manuscript online: June 16, 2021

Version of record online: July 20, 2021